12[th] IEA Heat Pump Conference 2017

Modeling and Experimental Investigations on Performance of Water Tanks in Circulating Heat Pump Water Heaters

Ruiqi Yang[a], Jun Pan[a], Bo Zheng[a,b], Xiangfei Liang[a,b]*, Rong Zhuang[a]

[a]*Gree Electric Appliances, Inc.of Zhuhai，Zhuhai 519070，China*
[b]*National Engineering Research Center of Green Refrigeration Equipment，Zhuhai 519070，China*

Abstract

The heat pump water heater (HPWH) is a promising technology due to its high performance and environment–friendliness. The water tank is an important part of a HPWH, and temperature distributions are essential in control strategy designing and assessment of the usable hot water volumes. This study aims to describe the effects of control strategies on temperature distributions in a water tank and the effects of flow rates on usable hot water volumes through CFD calculations and experiments. Results showed that the simulations were in good consistency with experiments and the temperature stratification was better in circulating heating for once than that for twice. A correlation was established to compute the real-time volume of usable hot water in a continuous water tapping.

Selection and/or peer-review under responsibility of the organizers of the 12th IEA Heat Pump Conference 2017.

Keywords: circulating HPWHs; water tank; modeling; experiments

1. Introduction

A heat pump water heater (HPWH) raises the water temperature to the setting value via a vapor-compression cycle and heat exchange in the condenser. Due to its high coefficient of performance and environment-friendliness, a HPWH has a more promising potential compared with an electric water heater and a gas water heater. The water tank is an important component of a circulating HPWH, and the temperature distributions are important in control strategy designing and assessment of the usable hot water volumes. Large quantities of experiments and system simulations involved in HPWHs [1~3] have been conducted already, and there are also several researches [4~7] about the temperature stratification in the tank, most of which concentrated on the tank structures' effects.

In this study, the effects of control strategies on temperature distributions in a water tank were researched through CFD simulations and experiments. Then the attempt was made to establish a correlation of the usable hot water volume based on the simulation results.

2. Water heating unit schematic

In general, a heat pump water heater system consists of two units, namely the heat pump unit and the water heating unit. Fig.1 showed the schematic of the water heating unit. As a main component, the water tank was connected to a water supplier, the users' terminal and the heat exchanger. More specifically, the tube connecting

* Corresponding author. Tel.: +86-756-866-8924.
E-mail address: liangxf@cn.gree.com.

the water tank and a water supplier was named water-in, and the tube connecting the water tank and the user's terminal was named water-out. The circulating-out and circulating-in tubes connected the tank and the heat exchanger together through switch valves. In the heating-up period, the water-out and circulating-out tubes acted as the circulating tubes for a better stratification and the other two tubes were out of use (the tubes which were not involved in heating-up period were shown in dash lines). The water heating unit was simplified to show a better understanding of the cyclic direction which was indicated by the arrows in this figure. During the heating-up period, the cold water was driven by a water pump, heated in the refrigerant-water heat exchanger (the condenser in the heat pump unit), and then returned to the top of the tank. Attention should be paid that the outlet direction of the water-out and circulating-out tubes were different. The volume of the cylinder tank was 191L with a height of 1810mm and an inner diameter of 370mm. The inner diameters of 4 connecting tubes were 14.4mm.

A flow meter was used to measure flow rates. 7 thermocouples were installed to measure the temperature distribution in the tank. They were carefully inserted into the blind holes whose ends were in the centre of the

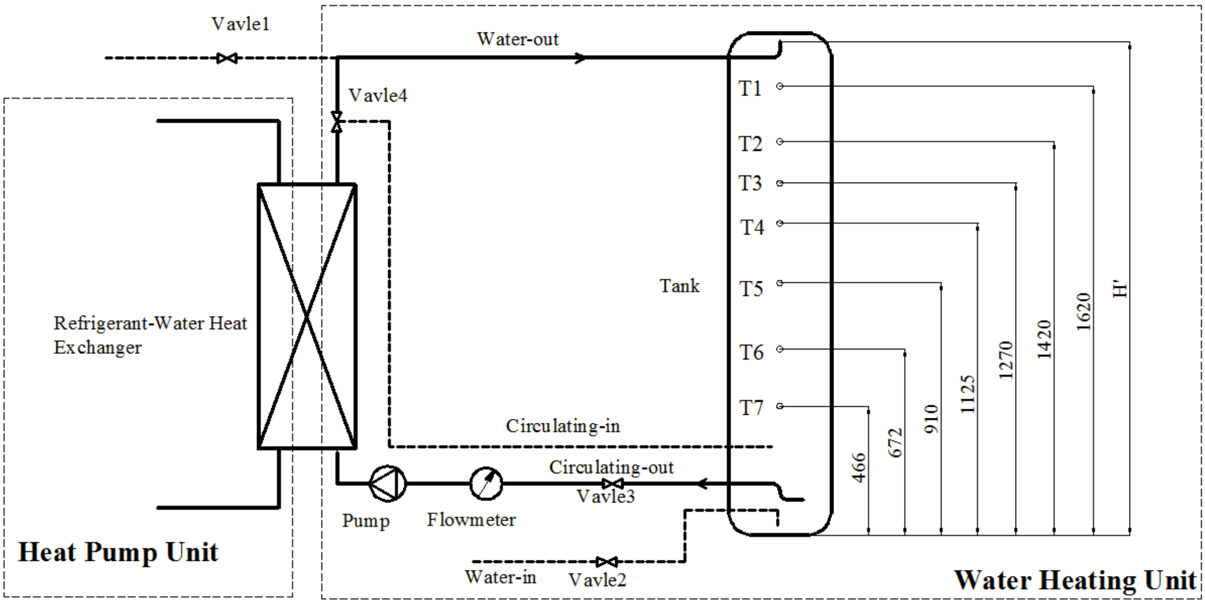

Fig. 1 The schematic of the water heating unit

cross sections. The heights from the bottom were 1620, 1420, 1270, 1125, 910, 672, and 466, respectively (units: mm).

The operating conditions were selected according to Chinese National Standard GB/T 23137-2008, shown in Table 1. Two control strategies were tested: circulating heating for once and for twice. Here, circulating heating for once meant the temperature of water increased to the setting value after flowing through the heat exchanger for only once. Circulating heating for twice meant the temperature of water increased to a medium value for the first time after getting heated in the condenser and then to the setting value for the second time. The nominal capacity of the heat pump was 3500W. The system was controlled as followings strategies. As to circulating heating for once, the initial cyclic flow rate was 1.083L/min and the inlet temperature of cyclic water was 55°C; the flow rate was adjusted to keep the inlet temperature constant as 55°C once the outlet temperature became higher than 9°C; the water was heated until the outlet temperature reached 39°C. As to circulating heating for twice, the flow rate was 2.167L/min until the inlet temperature reached 55°C, and it was adjusted to keep the inlet temperature stay at 55°C; test was finished when the outlet temperature reached 42°C. In order to keep the energy input constant, compressor frequency was adjusted during circulating heating for twice. The trigger temperatures, 39°C and 42°C, were designed lower than the setting values since the flow rates would increase rapidly to keep the inlet water temperature constant when the temperature differences in the heat exchanger were too small.

Table 1. Test conditions

	circulating heating for once	circulating heating for twice
Outdoor environmental temperature	7°C /6°C	7°C /6°C
Initial water temperature	9°C	9°C
maximal hot water temperature (the setting temperature)	55°C	55°C
Medium temperature	/	32°C
Final outlet temperature	39°C	42°C

3. CFD models description

The temperature distributions in the water tank were modeled using the commercial finite volume CFD solver, ANSYS Fluent 14.0. Integrated solver and implicit scheme were used to provide 3D unsteady state computation. Laminar was applied since the velocity in the tank was low enough. The pressure-velocity was coupled using SIMPLER model. The governing equations were discretised using the 2nd order upstream scheme. Properties of water were defined as the piecewise-linear functions of the temperature. The geometric model and the mesh of the computational zone were presented in Fig. 2. The tank was divided into several parts according to the sensors. Hex/Wedge mesh was adopted for middle part of the tank, while non-structured mesh was adopted for the rest parts.

For obtaining the grid independent modeling results, 5 meshes were tested, with 2897264, 771609, 539586, 399169, and 152409 cells, respectively. The test conditions were listed as following: (a) the initial temperature in the water tank was 9°C; (b) water circulated with an energy input of 3500W at a flow rate of 1.083L/min; (c) water flowed in and out through water-out and circulating-out tubes respectively. The number of time steps was set to 3600. Results were shown in Fig.2. Taking mesh1(2897264 cells) as a baseline, mesh2(771609) was selected for the later simulations as the result of a balance between accuracy and computational expense.

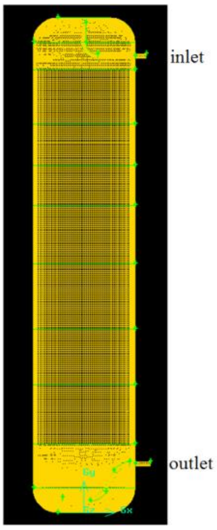

Fig.2 Geometric model and mesh for circulating heating

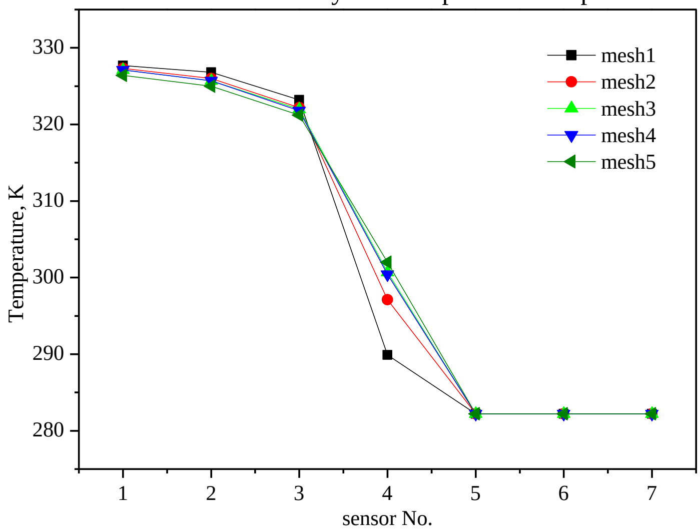

Fig.3 Results for grid independence test

In this study, circulating heating for once and for twice were simulated. The boundary conditions were listed as following: (a) the initial temperature in the water tank was 9°C; (b) the water flowed in and out through water-out and circulating-out tubes; (c) the inlet temperatures and flow rates were defined as:

$$
\begin{aligned}
& t = \frac{Q}{c_p Qv(t_{out},\tau)\rho} + T_{out} \\
& t < 55^{\mathrm{o}}\mathrm{C}, \quad T_{in} = t,\ Qv(T_{out},\tau) = Qv_0 \\
& t \geq 55^{\mathrm{o}}\mathrm{C}, \quad T_{in} = 55,\ \ Qv(T_{out},\tau) = Q / c_p / \rho / (T_{in} - T_{out})
\end{aligned}
\tag{1}
$$

Where, Q=3500W; Qv_0, the initial flow rates, was 1.083L/min and 2.167L/min for circulating for once and for twice, respectively. The temperature and flow rates were defined by UDFs.

Then an attempt to establish a correlation describing the real-time volume of usable hot water in a single tapping was made. The temperature differences were smaller than 5°C after placed statically for 2 hours, so it was rational to suppose that the initial temperature in the tank was uniform. Thus, the boundary conditions were: (a) the initial temperature in the water tank was 55°C and the inlet water temperature was 9°C; (b) the water was supplied through the water-in tube and flowed out through the water-out tube; (c) the flow rates were 4L/min, 6.67L/min and 9.55L/min for different cases.

4. Results and discussion

4.1. Circulating heating for once and for twice

Fig.4 showed the temperature distribution in the tank during circulating heat for once. The cold water was exported from the bottom, and reimported into the top of the tank after heated. The hot water took up the top of the tank and moved downwards gradually. A smaller temperature scale was used in the final image to make the distribution clear. The stratification in the tank was quite obvious during the whole heating-up period. Notice that the water in the bottom still remained cold at the end of the heating though most of the tank had been filled with hot water. The strategy that the outlet temperature of 39°C triggered the end of heating was designed for a higher coefficient of performance, but the final average temperature was lower than the setting value.

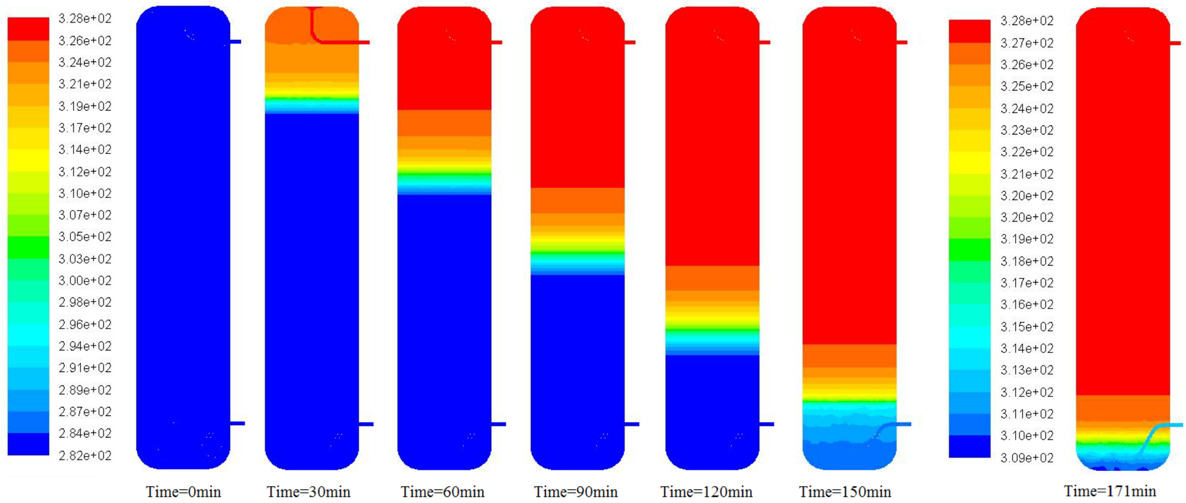

Fig.4 Temperature distribution in the tank during circulating heat for once

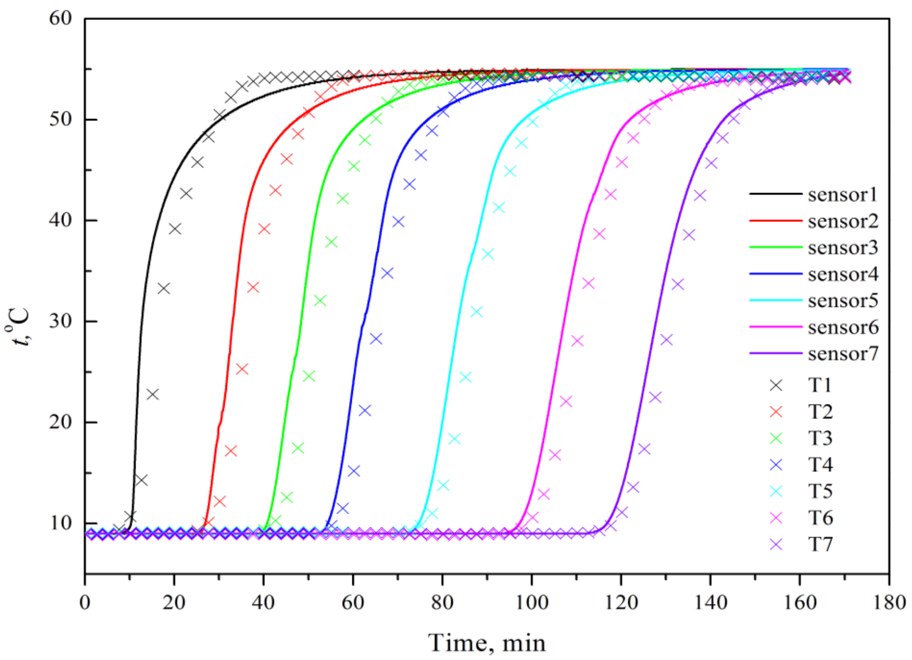

Fig.5 Curves of temperature during circulating heating for once

Fig.5 showed the temperature rising during circulating heating for once. The solid lines represented for simulation results and the crosses represented the experimental results. The total heating time was 171min, a little shorter than that in the experiment. The average temperatures of 7 levels rose successively, and the lower level's temperature remained almost constant even when the upper one had very closely reached the setting temperature. Heat transferred downwards with hot water, so the temperature of sensors rose rapidly as the hot water reached the levels. They changed slowly after they became higher than 50°C and finally all temperatures reached 55°C. The simulation was in good consistency with experimental results in the perspective view of the qualitative tendency. Several reasons may contribute to the quantitative errors besides the measurement accuracy: the CFD model was somehow over-simplified, ignoring the impacts of the circulating tubes and the blind holes of sensors; and the energy input of the heater in the start-up stage was rising gradually and was fluctuating in the experiment, while it was 3500W all over the simulation.

Fig.6 showed the temperature distribution during circulating heating for twice. With a higher cyclic flow rate, the cyclic inlet temperature was lower than that for once at the first stage, keeping as 32°C. The cyclic inlet temperature started to rise when the outlet temperature was higher than 9°C, and gradually came to 55°C, finally stayed 55°C as the result of flow rate adjustment. The temperature of water in the bottom remained lower than 55°C since the heating was finished when the outlet temperature reached 42°C, but it was higher compared with circulating heating for once. The stratification was clear as shown in the figure, though less significant compared to circulating heating for once.

Fig.7 showed comparisons of the sensors' temperature changes for both simulation and experiment. The heating period was divided into two stages and the curves in each stage were similar with that in circulating heating for once. At the end of the first stage, temperatures of all sensors reached 32°C. Then they gradually rose since the outlet temperature began to rise. The deviation between simulation and experiment was more significant than that in circulating heating for once. In addition to the reasons mentioned above, the adjustment delay of the compressor frequency was another important reason, especially in the second stage, since it was not high enough to keep the outlet temperature constant as expected.

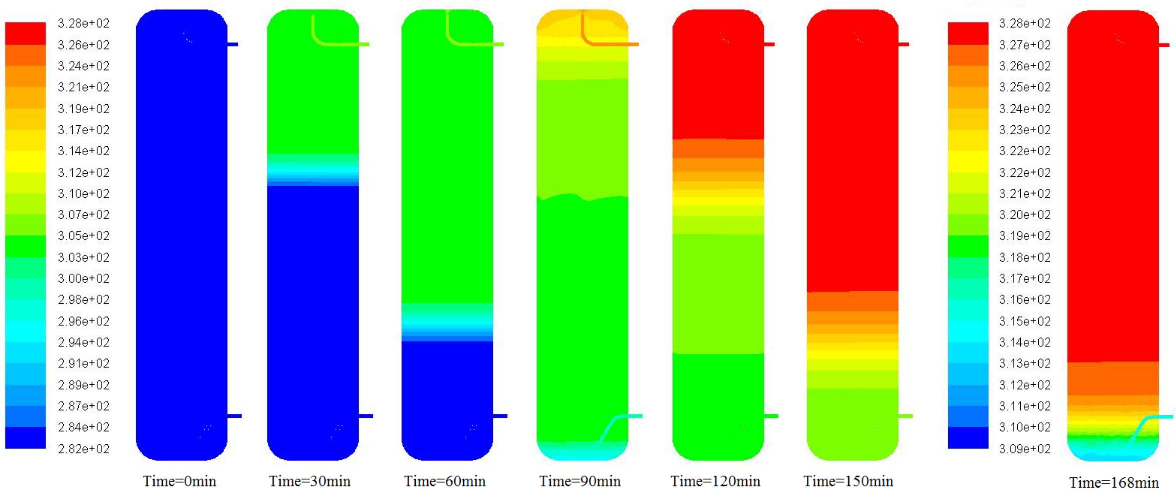

Fig.6 Temperature distribution in the tank during circulating heat for twice

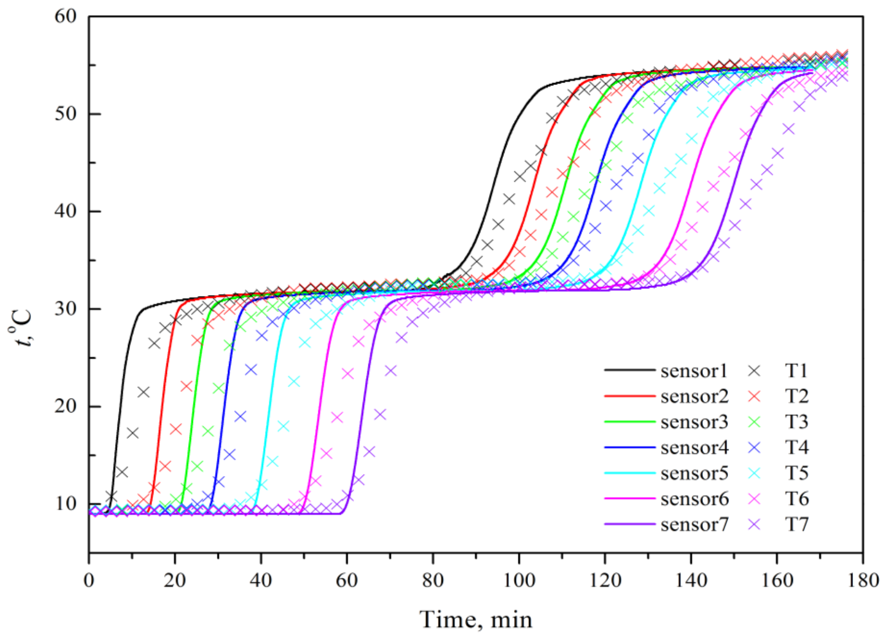

Fig.7 Comparisons of the sensors' temperature changes for both simulation and experiment

4.2. Correlations of real-time volume of usable hot water

Usable hot water volume is an important parameter to assessment the capacity of the water heater and is crucial to control strategy. According to Chinese National Standard, the usable hot water volume is defined as the volume of water with a temperature of less than 10°C below the setting temperature. In that case, the water with a temperature higher than 45°C was usable in this study. The volume of usable water was proportional to the height of 45°C isotherm level in most time and we concentrated on that mostly.

4.2.1. Simulation results

Fig.8 showed the height of 45°C isotherm levels *vs*. time for the 3 different flow rates. As predicted, the higher the flow rate was, the more rapidly the isotherm levels rose. The fluctuation at the beginning should be noticed. In fact, when the water injected into the tank, it would impinge on the bottom of the tank and then flowed around and upwards. In this period, the areas of isotherm levels were smaller than that of the cross section, and it was improper to be used to compute the volume of usable water. Another attention was drawn that the deviations from the average temperature in most regions and most time were quite small, as shown in Fig.9 (the flow rate was 9.55L/min). The significant differences appeared in the lower part of the tank ($H \leq 0.6$m) when the cold water reached their levels, which were due to the strong turbulence intensity in the inlet zone.

4.2.2. Modeling development

In the previous section, the details of 3D transient temperature distribution and the height of 45°C isotherm level in the tank were calculated using the CFD model. However, the curves were inconvenient to be used directly. As shown in the Fig.9, except for the mixing zone resulted from the injection of the inlet, the temperature distributions in cross sections were quite uniform in most locations along the height. So it was

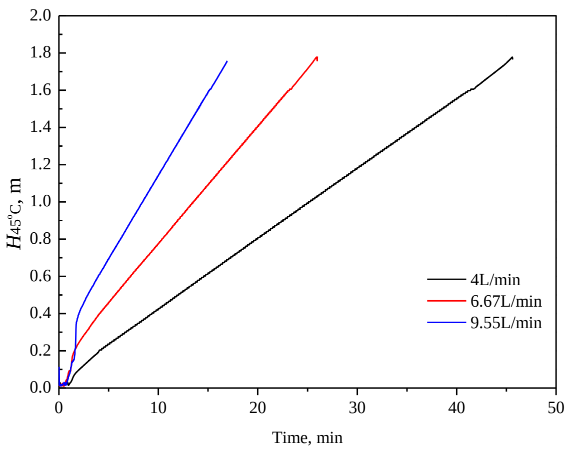

Fig.8 The height of 45°C isotherm levels

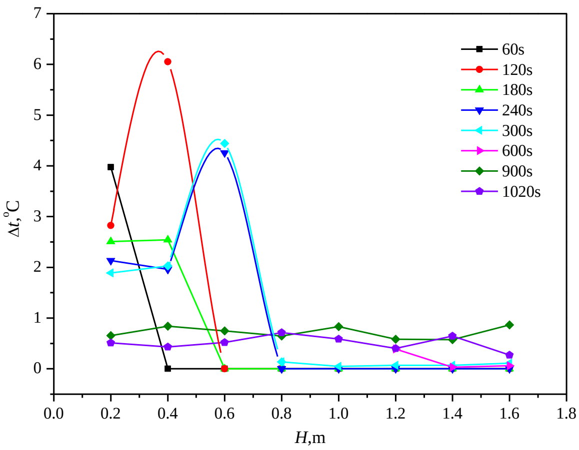

Fig.9 The deviations of temperature ($\Delta t=|t-t_{average}|_{max}$)

considerable to simplify that zone as a 1D zone. In this zone, the transient temperature profile averaged over the cross sections could be solved from the simplified one dimensional convection-conduction equation coupled with the known inlet fluid temperature as Eq. 2:

$$\frac{\partial t}{\partial \tau}+v\frac{\partial t}{\partial y}=a\frac{\partial^2 t}{\partial y^2} \quad (2)$$

For further simplification, two more assumptions were taken. First, it was assumed that the height of the tank was large enough so that the semi-infinite boundary condition can be applied for the outlet. Second, it was assumed that the mixing zone was small enough so that the inlet temperature of the 1D zone was equal to the injected temperature of the cold water. Then the initial and boundary condition were simplified as Eq. 3:

$$\begin{aligned} &\tau=0, t(y,0)=t_{hot} \\ &y=0, t(0,\tau)=t_{cold} \end{aligned} \quad (3)$$

Where t_{hot}=55°C, t_{cold}=9°C.Then the temperature profile turned out to be:

$$t(y,\tau)=\frac{(t_{hot}+t_{cold})}{2}+\frac{(T_{cold}-T_{hot})}{2}erf\,(\frac{y-v\tau}{2\sqrt{a\tau}}) \quad (4)$$

In order to get the correlation to compute the usable water volume, only the height of level $t(y,\tau)=45^{\mathrm{o}}\mathrm{C}$ was needed:

$$y = v\tau - 1.1048\sqrt{a\tau} = q_v\tau / A_{\mathrm{tank}} - 1.1048\sqrt{a\tau} \tag{5}$$

Where q_v was the flow rate and a was the thermal dissipation rate. Eq.5 was only suitable for the simplified model with neglect of the beginning stages. The impacts of the injection and the small area of the water-in tube had to be taken into consideration and the height of level t=45°C was amended as following:

$$H_{45^o\mathrm{C}} = q_v\tau / A_{\mathrm{tank}} - 1.1048\sqrt{a\tau} + C_1(C_2 - e^{-C_3\tau}) \tag{6}$$

Where C_1, C_2 and C_3 were constants related to inlet water flow rates, as listed in Table 2.

Table 2. Constants C_1, C_2 and C_3 in equation 6

q_v	9.55L/min	6.67L/min	4L/min
C_1	0.262	0.173	0.126
C_2	1	1.06	1.4
C_3	1.4633×10^{-2}	5.8333×10^{-3}	1.6667×10^{-4}

Using this analytical solution, the transient temperature profile along the height for the cold water injection stage can be calculated easily. The difference of the height between this simplified model and the full CFD results was smaller than 0.019m (*H'*=1.79m, *H'* was the distance between the water-out tube and the tank bottom, as defined in Fig.1.), which was acceptable for the preliminary engineering estimation. And the volume of usable water was:

$$Q_{usable} = (H' - H_{45^o\mathrm{C}})A_{\mathrm{tank}} \tag{7}$$

The beginning stages were not easy to compute since the height of 45°C isotherm levels was not available. In the beginning stages, the dominant heat transfer was convection rather than conduction, and the inlet flow rate was the main factor. So the volume of usable water was assumed to be in the form of:

$$Q_{usable} = H' A_{\mathrm{tank}} - C_4 q_v \tau \tag{8}$$

The turbulence intensity was enhanced as the flow rate was higher, so the constant C_4 and the period were different, too. Here, the beginning period, τ^*, was defined as the time when the 45°C isotherm levels were lower than the mixing zone. The C_4 and τ^* were listed in Table 3:

Table 3. Constants C_4, and τ^* in equation 8

q_v	9.55L/min	6.67L/min	4L/min
C_4	2.22255	1.65791	1.3132

τ*[unit: s]	104	178	240

So, the correlation of the usable water was:

$$Q_{usable} = \begin{cases} H' A_{\text{tank}} - C_4 q_v \tau, & \tau \le \tau * \\ (H' - H_{45^\circ\text{C}}) A_{\text{tank}}, & \tau > \tau * \end{cases} \tag{9}$$

And this correlation was only available in the continuous water tapping for the specific geometry of this tank, since the mixture of cold and hot water resulting from gravity was not taken into consideration, which is of great importance in the static stage.

5. Conclusions

The water tank is an important component in circulating heat pump water heaters. The temperature distribution and usable hot water quantities are key parameters in control strategy designing and assessment of water tanks. This paper studied the temperature distribution under circulating heating for once and for twice strategies through simulations and experiments. Then the correlation of real-time volume of usable hot water was established according to the simulation results. Conclusions are drawn as followings:

1) The simulation results were in good consistency with experiments. Temperature distributions were quite different under the two different control strategies. The stratification was better in circulating heating for once than that for twice.

2) Usable hot water volumes under different flow rates were simulated and a correlation was established to compute the usable hot water volumes.

References

[1]K. Hudon, B. Sparn, D. Christensen, etc. Heat Pump Water Heater Technology Assessment Based on Laboratory Research and Energy Simulation Models, ASHRAE Winter Conference, Chicago, Illinois, January 21-25, 2012.

[2] A. Hepbasli, Y. Kalinci. A review of heat pump water heating systems, Renewable and Sustainable Energy Reviews, 2009 (13) 1211–1229.

[3] L. Yang, H.Yuan, J. Peng, C.Zhang. Performance modeling of air cycle heat pump water heater in cold climate, Renewable Energy, 87 (2016) 1067-1075.

[4] A. Pizzolato, F. Donato, V. Verda, M. Santarelli. CFD-based reduced model for the simulation of thermocline thermal energy storage systems, Applied Thermal Engineering, 76 (2015) 391-399.

[5] L. J. Shah, E. Andersen, S. Furbo. Theoretical and experimental investigations of inlet stratifiers for solar storage tanks, Applied Thermal Engineering 25 (2005) 2086–2099.

[6] W. Yaïci, M. Ghorab, E. Entchev, S. Hayden. Three-dimensional unsteady CFD simulations of a thermal storagetank performance for optimum design, Applied Thermal Engineering, 60 (2013) 152-163.

[7] Y. Li, S. Li, M. Zhao,X. Zhang. Simulation and Experimental Investigation of the Influence onthe Performance of Tanks with Different Inlets, Journal of refrigeration, 34 (2013) 13-16.